Universal Negative Poisson Ratio of Self-Avoiding Fixed-Connectivity Membranes

M. Bowick,[1] A. Cacciuto,[1] G. Thorleifsson,[2] and A. Travesset[3]
[1]*Physics Department, Syracuse University, Syracuse, New York 13244-1130*
[2]*DeCODE Genetics, Lynghalsi 1, 1S-110, Reykjavik, Iceland*
[3]*Loomis Laboratory, University of Illinois at Urbana, Urbana, Illinois 61801*
(Received 7 March 2001; published 14 September 2001)

We determine the Poisson ratio of *self-avoiding* fixed-connectivity membranes, modeled as impenetrable plaquettes, to be $\sigma = -0.37(6)$, in statistical agreement with the Poisson ratio of *phantom* fixed-connectivity membranes $\sigma = -0.32(4)$. Together with the equality of critical exponents, this result implies a *unique* universality class for fixed-connectivity membranes. Our findings thus establish that physical fixed-connectivity membranes provide a wide class of *auxetic* (negative Poisson ratio) materials with significant potential applications in materials science.

DOI: 10.1103/PhysRevLett.87.148103 PACS numbers: 87.16.Dg, 82.70.Uv, 87.16.Ka

Fixed-connectivity (also known as polymerized, tethered, or crystalline) membranes are fluctuating and flexible fishnetlike two-dimensional surfaces with nodes of a fixed coordination number (for two recent reviews, see [1,2]). Physical examples include such naturally occurring structures as polymerized Langmuir-Blodget films [3,4] and the spectrin/actin cytoskeleton [5] of erythrocytes (mammalian red blood cells). A wide variety of additional examples is discussed in [1]. Current advances in soft condensed matter experimental techniques suggest the likelihood of many new realizations of fixed-connectivity membranes such as cross-linked DNA networks as well as composite structures that include fixed-connectivity membranes as fundamental ingredients. One universal and remarkable feature of the low-temperature (so-called *flat*) phase of non-self-avoiding (*phantom*) fixed-connectivity membranes is that they expand transversely when stretched longitudinally [6–9]. In other words, they exhibit a negative Poisson ratio [10]. Such materials have been dubbed *auxetic* [11].

In this Letter we estimate, via Monte Carlo simulations, the Poisson ratio of physical *self-avoiding* fixed-connectivity membranes. We establish that they are *also* auxetic materials with a Poisson ratio and roughness exponent in statistical agreement with those of flat phantom membranes. Thus there appears to be a unique universality class of flat fixed-connectivity membranes, whether they arise from high bending rigidity or self-avoidance. Direct experimental measurements should be able to measure this negative Poisson ratio and test universality. The remarkable properties of auxetic membranes suggest a rich new avenue of exploration in materials synthesis.

A fixed-connectivity membrane may be modeled as an elastic surface with bending rigidity and self-avoidance [12–15]. The free energy is composed of an elastic and a self-avoiding contribution:

$$F_{\mathrm{fcm}} = F_{\mathrm{el}} + F_{\mathrm{sa}}\,. \tag{1}$$

The elastic free energy F_{el} is given by

$$F_{\mathrm{el}}(\mathbf{u}, h) = \int d^2\mathbf{x}\left[\frac{\kappa}{2}(\partial_\alpha\partial_\beta h)^2 + \mu u_{\alpha\beta}^2 + \frac{\lambda}{2}u_{\alpha\alpha}^2\right], \tag{2}$$

where $\mathbf{u}$ denotes phonon modes, h denotes height modes, κ is the bending rigidity, and λ and μ are the classical Lamé coefficients. The self-avoiding free energy we take to be of the Edwards form

$$F_{\mathrm{sa}} = \frac{b}{2}\int d^2\mathbf{x}\int d^2\mathbf{y}\,\delta^3[\vec{r}(\mathbf{x}) - \vec{r}(\mathbf{y})], \tag{3}$$

where b determines the strength of self-avoidance. The strain tensor $u_{\alpha\beta}$ [10] is related to the embedding $\vec{r}(\mathbf{x})$, defining the membrane by

$$\begin{aligned}\vec{r}(\mathbf{x}) &= \mathbf{x} + \mathbf{u}(\mathbf{x}) + \hat{z}h(\mathbf{x})\,,\\ u_{\alpha\beta} &= \frac{1}{2}(\partial_\alpha u_\beta + \partial_\beta u_\alpha + \partial_\alpha h\partial_\beta h)\,.\end{aligned} \tag{4}$$

Combined efforts both on the analytical and the numerical side have led to a complete clarification of the phase diagram of the *phantom* case ($b = 0$) and detailed estimates for the critical exponents, as shown in Fig. 1 and Table I. The phase diagram consists of a crumpled phase [associated with the Gaussian fixed point (GF)] and a flat phase [associated with a flat phase fixed point (FL)], with an intermediate infrared-unstable crumpling transition (CT), as depicted in Fig. 1.

The self-avoiding model of Eq. (1) with no bending rigidity ($\kappa = 0$) has proven to be tractable numerically [16]. The model possesses a unique infrared fixed point (SA) describing a flat phase, with detailed results for critical exponents given in Table I. From the analytical standpoint there is evidence for a unique SA [17,18], but the calculations are inconclusive on whether it describes a flat or a crumpled phase [19–24].

A look at Table I reveals that the critical exponents and the Poisson ratio of both phantom and self-avoiding membranes coincide within the error bars quoted, implying that the FL and the SA are equivalent. This is a very surprising result since it means that the same long wavelength limit

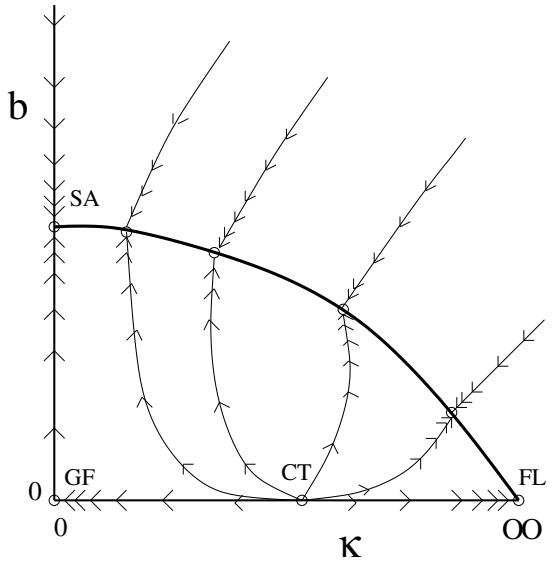

FIG. 1. The renormalization group flows in the two-dimensional space of couplings for a fixed-connectivity membrane with bending rigidity (κ) and self-avoidance (b). The phantom model ($b = 0$) has two infrared-stable fixed points, the crumpled phase (GF) and the flat phase (FL), with an intermediate continuous crumpling transition associated with the infrared-unstable fixed point (CT). The pure self-avoiding model with no microscopic bending rigidity ($\kappa = 0$) has an infrared stable self-avoiding fixed point (SA). There is a line of equivalent fixed points joining the FL and the SA (the solid line), thus defining a redundant direction in κ-b space.

is reached via two very different routes: either sufficiently large bending rigidity or strong self-avoidance in the absence of bending rigidity. This is even more remarkable considering the very different short-distance structure of the two models: a membrane with large bending rigidity is very smooth at short distances while a purely self-avoiding membrane in the absence of bending rigidity is extremely rough.

In light of our results, we suggest the renormalization group (RG) flows depicted in Fig. 1. Given these flows and the equivalence of the SA and the FL, there must be a full line of equivalent fixed points $b(\kappa)$ joining them, with no RG flow on the line (corresponding to a marginal direction). Since these are the infrared-stable fixed points of the system, all the relevant physics are described by this line. The crumpling transition present for phantom membranes may be reached only by an extremely precise tuning of the parameters involved in the problem. This would make the crumpling transition in the model described as very difficult to verify experimentally.

TABLE I. Critical exponents and Poisson ratio of flat fixed-connectivity membranes in the phantom (MC: Monte Carlo; SCSA: self-consistent screening approximation) and the self-avoiding case (MC-BS: Monte Carlo with Balls and Springs models; MC-IP: Monte Carlo with impenetrable models).

		Phantom		
	MC	ε expansion	SCSA	Large d
ν	0.95(5) [25]	1	1	1
ζ	0.64(2) [25]	13/25 [6]	0.59 [7]	2/3 [26]
σ	−0.32(4) [9]	−1/5 [6]	−0.33 [6]	
		Self-avoiding		
	MC-BS	MC-IP	Experiments	
ν	1 [27]	0.97(4) [16]	0.93(5) [28]	
ζ	0.65 [27]	0.64(2) [16]	0.65(10) [5]	
σ		−0.37(6)		

We see that the combination of fixed connectivity (integrity of the lattice) and self-avoidance sufficiently restricts the entropy of crumpled configurations as to destroy the crumpled phase. It was already observed in [29] that next-to-nearest neighbor self-avoidance, discretized by hard-sphere potentials, induces a positive bending rigidity. On the other hand, the impenetrable plaquette model treated here is very flexible, since only strictly self-intersecting configurations are forbidden, and hence the physical mechanism flattening the membrane is clearly more general than the simple induced bending rigidity discussed above.

We performed a Monte Carlo simulation of a suitable discrete version of the model [Eq. (1)], as described in [16]. The Poisson ratio σ for a two-dimensional system deformed from its mean length l by δl is determined by

$$\sigma = -\frac{\delta w/w}{\delta l/l}, \tag{5}$$

where $\delta w/w$ measures the fractional change in the transverse extent (width) of the system. In [9] it is shown that linear response theory gives

$$\sigma = -\frac{\langle \overline{u}_{xx}\overline{u}_{yy}\rangle_c}{\langle \overline{u}_{yy}^2\rangle_c}, \tag{6}$$

where $\langle u^2\rangle_c$ is the connected statistical average over Monte Carlo configurations and $\overline{u}$ is the spatial average over the surface.

Our results are presented in Fig. 2(A) and show that the Poisson ratio $\sigma = -1/3$ obtained in simulations of flat phantom fixed-connectivity membranes is also a good estimate of the Poisson ratio for the pure self-avoiding model. Error bars have been calculated with the Jacknife method [30,31].

To calibrate the influence of the boundary on our results we calculated the Poisson ratio excluding concentric outer shells of nodes neighboring the boundary. In particular, we performed the numerical analysis discarding shells of boundary nodes of increasing extent. The results are presented in Fig. 2(B).

The exclusion of larger shells of boundary sites slightly increases the absolute value of the Poisson ratio. For sufficiently small reduced linear size, $|\sigma|$ begins to decrease due to finite size effects. There is consequently competition between boundary and finite size effects. Finite size effects become important only when a sizable fraction of nodes near the boundary is excluded. Note that we can also

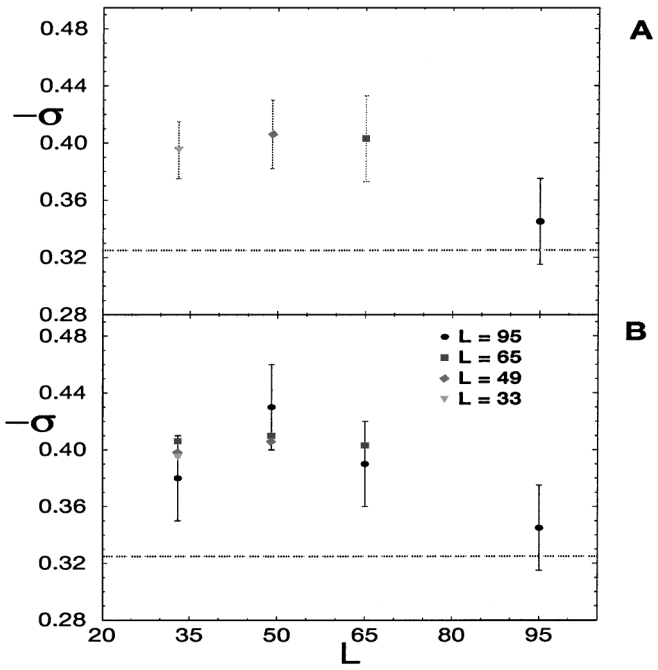

FIG. 2. Poisson ratio of a self-avoiding fixed-connectivity membrane as a function of system size (A). Poisson ratio of reduced lattices compared with nontruncated ones (B). The straight dashed line indicates in both cases the SCSA analytical result $\sigma = -1/3$.

make a consistent check of our analysis by systematically excluding shells of nodes from the boundary in towards the center of the lattice and comparing the lattices of reduced size thus obtained with equal volume nontruncated lattices.

Thus we can compare, for example, the $L = 65$ result with that from the reduced $L = 95$ lattice and likewise the $L = 49$ result with that from the reduced $L = 95$ and $L = 65$ lattices. The matching given by this comparison is consistent. In fact we are able to reproduce the $L = 65$, $L = 49$, and $L = 33$ results simply by reducing the $L = 95$ lattice. The deviations found in this comparison are another measure of boundary effects.

Traditional materials get thinner when stretched and fatter when squashed, since it is typically difficult to increase their volume very much when deformed. (A volume preserving deformation has a Poisson ratio of 0.5. Any value less than 0.5 involves some increase in volume under deformation. A negative Poisson ratio implies a very large volume increase.) In the unusual world of auxetics the opposite happens, with a number of interesting implications and potential applications. There are several well-known auxetic materials. The earliest example, dating from more than a century ago, is that of a pyrite crystal [32], which has a Poisson ratio in certain directions of $\sigma \sim -0.14$. More recently some polyester foams under certain pressure conditions have proved to be isotropic auxetic materials with Poisson ratios as large as $\sigma \sim -0.7$ [33]. A nice mechanical model for auxetic materials was given in [11] (see Fig. 3). One of the rare naturally occurring auxetics is SiO_2 in its α-crystobalite phase [34,35].

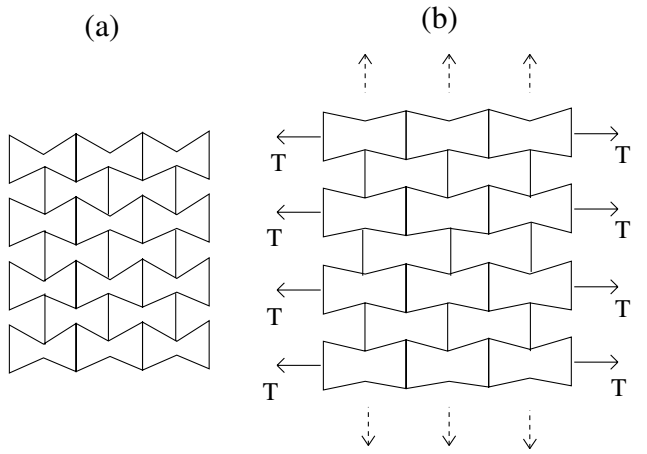

FIG. 3. Mechanical model of an auxetic material: (a) in the absence of applied stress and (b) under applied lateral stress T. The lateral stretching accompanying the applied stress forces the material out in the transverse dimension.

The underlying mechanism driving fixed-connectivity membranes auxetic has some similarities to that illustrated in Fig. 3. Submitting a membrane to tension will suppress its out-of-plane fluctuations, forcing it entropically to expand in both in-plane directions. More physically, the out-of-plane undulations renormalize the elastic constants (the Lamé coefficients), in such a way that the long wavelength bulk modulus is less than the shear modulus, which is the signature of a two-dimensional auxetic material.

Auxetic materials have desirable mechanical properties such as higher in-plane indentation resistance, transverse shear modulus, and bending stiffness. They have clear applications as sealants, gaskets, and fasteners. They may also be promising materials for artificial arteries, since they can expand to accommodate sudden increases in blood flow.

We can model a realistic fixed-connectivity membrane with an elastic free energy and either large bending rigidity or self-avoidance. This is of practical importance in modeling since, for example, we may replace the more complicated nonlocal self-avoidance term with a large bending rigidity. It remains an important theoretical challenge to verify this conclusion analytically.

In this Letter we have ignored the role of topological defects. We think that a sufficiently large defect density may affect the actual value of the Poisson ratio, but a detailed discussion of this topic is beyond the scope of this paper.

It is our hope that the results presented in this Letter will encourage materials scientists and condensed matter experimentalists to further study the elastic and mechanical properties of fixed-connectivity membranes and, in particular, to measure the Poisson ratio of these novel systems.

The work of M. B., A. C., and A. T. has been supported by the U.S. Department of Energy (DOE) under Contract No. DE-FG02-85ER40237. A. T. acknowledges funding from the materials computation center, Grant No. NSF-DMR 99-76550 and NSF Grant No. DMR-0072783.

[1] M. Bowick and A. Travesset, in *Renormalization Group Theory at the Turn of the Millennium,* edited by D. O'Connor and C. R. Stephens [Phys. Rep. **344**, 255 (2001)].
[2] K. J. Wiese, *Polymerized Membranes, a Review,* edited by C. Domb and J. L. Lebowitz, Phase Transitions and Critical Phenomena Vol. 19 (Academic Press, New York, 2001), pp. 253–480.
[3] J. H. Fendler and P. Tundo, Acc. Chem. Res. **17**, 3 (1984).
[4] J. H. Fendler, Chem. Rev. **87**, 877 (1987).
[5] C. F. Schmidt, K. Svoboda, N. Lei, I. B. Petsche, L. E. Berman, C. R. Safinya, and G. S. Grest, Science **259**, 952 (1993).
[6] J. A. Aronovitz and T. C. Lubensky, Phys. Rev. Lett. **60**, 2634 (1988).
[7] P. Le Doussal and L. Radzihovsky, Phys. Rev. Lett. **69**, 1209 (1992).
[8] Z. Zhang, H. T. Davis, and D. M. Kroll, Phys. Rev. E **53**, 1422 (1996).
[9] M. Falcioni, M. J. Bowick, E. Guitter, and G. Thorleifsson, Europhys. Lett. **38**, 67 (1997).
[10] L. D. Landau and E. M. Lifshitz, *Theory of Elasticity,* Course of Theoretical Physics Vol. 7 (Pergamon Press, Oxford, U.K., 1986).
[11] K. E. Evans, M. A. Nkansah, I. J. Hutchinson, and S. C. Rogers, Nature (London) **353**, 124 (1991).
[12] Y. Kantor, M. Kardar, and D. R. Nelson, Phys. Rev. Lett. **57**, 791 (1986).
[13] D. R. Nelson and L. Peliti, J. Phys. (Paris) **48**, 1085 (1987).
[14] Y. Kantor, M. Kardar, and D. R. Nelson, Phys. Rev. A **35**, 3056 (1987).
[15] M. Paczuski, M. Kardar, and D. R. Nelson, Phys. Rev. Lett. **60**, 2638 (1988).
[16] M. Bowick, A. Cacciuto, G. Thorleifsson, and A. Travesset, Eur. Phys. J. E **5**, 149 (2001).
[17] B. Duplantier, Phys. Rev. Lett. **58**, 2733 (1987).
[18] M. Kardar and D. R. Nelson, Phys. Rev. Lett. **58**, 1289 (1987).
[19] T. Hwa, Phys. Rev. A **41**, 1751 (1990).
[20] E. Guitter and J. Palmeri, Phys. Rev. A **45**, 734 (1992).
[21] M. Goulian, J. Phys. II (France) **1**, 1327 (1991).
[22] P. Le Doussal, J. Phys. A **25**, L469 (1992).
[23] F. David and K. J. Wiese, Phys. Rev. Lett. **76**, 4564 (1996).
[24] K. J. Wiese and F. David, Nucl. Phys. **B487**, 529 (1997).
[25] M. J. Bowick, S. M. Catterall, M. Falcioni, G. Thorleifsson, and K. N. Anagnostopoulos, J. Phys. I (France) **6**, 1321 (1996).
[26] F. David and E. Guitter, Europhys. Lett. **5**, 709 (1988).
[27] F. F. Abraham and D. R. Nelson, Science **249**, 393 (1990).
[28] M. S. Spector, E. Naranjo, S. Chiruvolu, and J. A. Zasadzinski, Phys. Rev. Lett. **73**, 2867 (1994).
[29] F. F. Abraham and D. R. Nelson, J. Phys. (Paris) **51**, 2653 (1990).
[30] B. Efron, *The Jacknife, the Bootstrap and Other Resampling Plans* (SIAM, Philadelphia, PA, 1982).
[31] J. Shao and D. Tu, *The Jackknife and Bootstrap* (Springer, New York, 1995).
[32] A. E. H. Love, *A Treatise on the Mathematical Theory of Elasticity* (Dover, New York, 1944), 4th ed., p. 163.
[33] R. Lakes, Science **235**, 1038 (1987).
[34] D. J. Weidner, A. Yeganeh-Haeri, and J. B. Parise, Science **257**, 650 (1992).
[35] N. Keskar and J. R. Chelikowsky, Nature (London) **358**, 222 (1992).